Biomaterials 34 (2013) 5496–5505

Contents lists available at SciVerse ScienceDirect

Biomaterials

journal homepage: www.elsevier.com/locate/biomaterials

Engineered cell-laden human protein-based elastomer

Nasim Annabi [a,b,c], Suzanne M. Mithieux [d], Pinar Zorlutuna [a,b,g], Gulden Camci-Unal [a,b], Anthony S. Weiss [d,e,f,**], Ali Khademhosseini [a,b,c,*]

[a] Center for Biomedical Engineering, Department of Medicine, Brigham and Women's Hospital, Harvard Medical School, Boston, MA 02139, USA
[b] Harvard-MIT Division of Health Sciences and Technology, Massachusetts Institute of Technology, Cambridge, MA 02139, USA
[c] Wyss Institute for Biologically Inspired Engineering, Harvard University, Cambridge, MA 02139, USA
[d] School of Molecular Bioscience, University of Sydney, Sydney 2006, Australia
[e] Bosch Institute, University of Sydney, Sydney 2006, Australia
[f] Charles Perkins Centre, University of Sydney, Sydney 2006, Australia
[g] Biomedical Engineering Program and Mechanical Engineering Department, University of Connecticut, 191 Auditorium Road, Storrs, CT 06269-3139, USA

ARTICLE INFO

Article history:
Received 6 February 2013
Accepted 23 March 2013
Available online 29 April 2013

Keywords:
Elastin
Photocrosslinking
Cell-laden hydrogel
Tropoelastin
Elastomer

ABSTRACT

Elastic tissue equivalence is a vital requirement of synthetic materials proposed for many resilient, soft tissue engineering applications. Here we present a bioelastomer made from tropoelastin, the human protein that naturally facilitates elasticity and cell interactions in all elastic tissues. We combined this protein's innate versatility with fast non-toxic fabrication techniques to make highly extensible, cell compatible hydrogels. These hydrogels can be produced in less than a minute through photocrosslinking of methacrylated tropoelastin (MeTro) in an aqueous solution. The fabricated MeTro gels exhibited high extensibility (up to 400%) and superior mechanical properties that outperformed other photocrosslinkable hydrogels. MeTro gels were used to encapsulate cells within a flexible 3D environment and to manufacture highly elastic 2D films for cell attachment, growth, and proliferation. In addition, the physical properties of this fabricated bioelastomer such as elasticity, stiffness, and pore characteristics were tuned through manipulation of the methacrylation degree and protein concentration. This photocrosslinkable, functional tissue mimetic gel benefits from the innate biological properties of a human elastic protein and opens new opportunities in tissue engineering.

1. Introduction

The golden standard for elastic tissue engineering is a moldable, substantially elastic, biologically compatible, human-based protein polymer that provides for the encapsulation and surface growth of multiple cell types [1–3]. Available elastomers include polysiloxanes [4,5], polyurethanes [6,7], polyhydroxyalkanoates [8,9], poly(diol citrates) [10], poly(glycerol-sebacate) [11,12], and hybrid alginate/polyacrylamide [13]. These artificial chemical elastomers have some limitations. For example, they may require high temperatures and cytotoxic agents in their synthesis making them incompatible with viable cell encapsulation. They also do not possess the innate ability to bind cells and require artificial derivatization to address this deficiency. In addition, the general release of toxic components during breakdown *in vivo* stand in the way of their broad approval as implantable materials in humans [11–14].

We used a biomimetic approach to make a new class of engineered elastic materials by drawing on elastin's ubiquitous, functional persistence in human elastic tissues. Elastin is required to maintain structural integrity, confer elasticity, and signal cells to coordinate their activities. For example, blood vessels, skin, heart, lung, bladder, and elastic cartilage all contain elastin. Tropoelastin is the natural monomeric precursor of elastin. We took the perspective that materials based on recombinant tropoelastin would yield elastic tissue equivalents if the protein could be photocrosslinked in less than a minute.

Most elastin is formed in the womb with the slow crosslinking of tropoelastin following its lysine-specific oxidation by lysyl oxidase. Various crosslinking approaches have been used to produce three dimensional (3D) elastin-based hydrogels from recombinant human tropoelastin [15,16], α-elastin [17–19], and engineered elastin-like polypeptides (ELPs) [20–22]. The resulting hydrogels generally show biocompatibility and support cell growth both *in vitro* and

* Corresponding author. Center for Biomedical Engineering, Department of Medicine, Brigham and Women's Hospital, Harvard Medical School, Boston, MA 02139, USA.
** Corresponding author. School of Molecular Bioscience, University of Sydney, Sydney 2006, Australia.
E-mail addresses: alik@rics.bwh.harvard.edu, alik@mit.edu (A. Khademhosseini).

0142-9612/$ – see front matter © 2013 Elsevier Ltd. All rights reserved.
http://dx.doi.org/10.1016/j.biomaterials.2013.03.076

in vivo; however, low mechanical properties [23,24] and a non-homogenous cell penetration into the 3D structures of these hydrogels [15] are issues. Furthermore, the use of cytotoxic conditions including chemical crosslinkers [15,25], organic solvents [18,26], prolonged UV exposure [27] and high pressure [17,19] in the fabrication of these hydrogels prevents viable cell encapsulation during hydrogel formation.

To address these challenges, we used a synthetic path to generate highly elastic 3D cell-laden tropoelastin-based hydrogels by brief, light-initiated crosslinking of methacrylated tropoelastin (MeTro). The use of recombinant human tropoelastin containing 35 lysine residues per molecule was expected to promote cell-adhesive properties of the engineered construct. We hypothesized that our approach may enable us to control the physical properties of fabricated elastic hydrogels, such as pore characteristics, swelling behavior, and mechanical properties by changing the methacrylation degree and polymer concentration. *In vitro* studies were also conducted to assess the suitability of the MeTro gel for both 3D elastic environments for cell encapsulation and 2D films for surface growth of multiple cell types.

2. Materials and methods

2.1. Tropoelastin synthesis

Recombinant human tropoelastin isoform SHELΔ26A (Synthetic Human Elastin without domain 26A) corresponding to amino acid residues 27–724 of GenBank entry AAC98394 was purified from *Escherichia coli* on a multi-gram scale using fermentation, selective alcohol solubilization, and reverse phase HPLC methodologies as previously described [28,29]. SHELΔ26A represents the 60 kDa mature form of the most frequently observed secreted splice form of the protein following removal of the signal peptide.

2.2. MeTro synthesis and characterization

Tropoelastin was methacrylated by the addition of methacrylate anhydride (MA, Sigma) to a 10% (w/v) tropoelastin solution in phosphate buffered saline (PBS; Invitrogen) and reacted for 12 h at 4 °C. The solution was then diluted and dialyzed (Slide-A-Lyzer MINI, 3.5K MWCO) against distilled water at 4 °C for 48 h and lyophilized to yield MeTro. Various concentrations of MA (e.g. 8, 15, 20% (v/v)) were used to influence the degree of methacrylation. ^{1}H NMR analysis was used to calculate the methacrylation degree of MeTro. The effect of methacrylation on the coacervation behavior and secondary structure of tropoelastin was investigated using UV spectrophotometry and circular dichroism (CD) analysis, respectively.

2.2.1. ^{1}H NMR

^{1}H NMR spectra of tropoelastin and MeTro solutions in D_2O (1% (w/v)) were obtained on a Varian Inova-500 NMR spectrometer and used to calculate the extent of methacrylation. NMR was performed at 4 °C to prevent coacervation of MeTro solutions during analysis. The degree of methacrylation was calculated using the peak values between 4.9 and 6 ppm from methacrylate groups and the peak at 2.6 ppm from lysine residues in tropoelastin and defined as the number of methacrylated lysines divided by the total number of lysines.

2.2.2. UV spectrophotometry

The coacervation behavior of 1% (w/v) tropoelastin and MeTro solutions in PBS were assayed by monitoring turbidity through light scattering (300 nm) using a spectrophotometer (Shimadzu UV-1601). The turbidity of each solution was assayed for 10 min at temperatures ranging from 4 °C to 45 °C. The temperature was controlled by connecting the cuvette holder to a recirculating water bath. To investigate the effect of methacrylation degree on coacervation behavior, MeTro macromers with varying methacrylation degrees were used. Following each measurement, the solutions were cooled to 4 °C for 10 min. At each temperature, the maximum variation in turbidity was recorded and expressed as a percentage of maximum turbidity for each MeTro solution to generate a series of coacervation curves.

2.2.3. Circular dichroism

Tropoelastin and MeTro samples were dissolved in water at 0.015% (w/v) and monitored using 0.1 cm quartz cuvettes in a Jasco J-815 CD spectrometer. Five spectral accumulations were obtained for each sample. Spectra were measured from 184 to 240 nm at 20 °C. Data were expressed in terms of the mean residue ellipticity (deg cm^2 dmol^{-1}). Secondary structure analysis of the CD spectra was performed with CONTIN, SELCON3 and CDSSTR programs through the CDPro software package using reference set SP43 [30].

2.3. Hydrogel fabrication and characterization

MeTro macromers with different degrees of methacrylation were used to make photocrosslinked MeTro hydrogels. To prepare the hydrogels, various concentrations of MeTro solutions (e.g. 5, 10, 15% (w/v)) were prepared in PBS containing 0.5% (w/v) 2-hydroxy-1-(4-(hydroxyethoxy) phenyl)-2-methyl-1-propanone (Irgacure 2959, CIBA Chemicals) at 4 °C. Photocrosslinked MeTro gel was formed by pipetting 10 μl of the solution between two glass coverslips that were separated by a 150 μm spacer and exposing to 6.9 mW/cm^2 UV light (360–480 nm) for 35 s. MeTro solutions with varying methacrylation degrees were used to examine the effects of the extent of methacrylation on hydrogel characteristics including pore architecture, swelling ratio, and tensile and compressive properties. GelMA hydrogels were prepared by using 10% (w/v) GelMA with 80% methacrylation degree as previously described [31] and used as controls for mechanical properties characterization. Poly (ethylene glycol) dimethacrylate (PEGDMA, MW 1000 Da) hydrogels were also formed [32] and used as controls for the *in vitro* studies.

2.3.1. Swelling ratio

The swelling behavior of MeTro hydrogels was evaluated at 37 °C in PBS using previously reported procedures [17,25]. To prepare MeTro hydrogels for swelling ratio measurements, 40 μL MeTro solution was first injected into a custom-made polydimethylsiloxane (PDMS) mold (diameter: 5 mm and depth: 1 mm). A glass coverslip was placed on the mold before exposing to UV light for 180 s. Samples were then collected from the mold and detached from the slide after soaking in PBS for 5 min. To calculate swelling ratios, the gels were lyophilized and their dry weights were recorded. The samples were then incubated in PBS for 24 h after which the excess liquid was removed from the swollen gels and the samples were reweighed. The swelling ratio was then calculated as the ratio of mass increase to the mass of dry samples. The effect of methacrylation degree and MeTro concentrations on the swelling ratio was obtained. At least 5 samples were tested for each condition.

2.3.2. Scanning electron microscopy (SEM)

SEM analysis was used to determine the pore characteristics of the fabricated MeTro hydrogels and also to examine cell growth on the surfaces of hydrogels. SEM images of MeTro gels were obtained by using a FEI/Philips XL30 FEG SEM (15 KV). Lyophilized samples were mounted on aluminum stubs and gold coated prior to SEM analysis. The effects of methacrylation degree and polymer concentrations on the pore characteristics of MeTro hydrogels were examined. The average pore sizes of fabricated MeTro gels were calculated using ImageJ software. For pore size measurement, at least 100 pores were measured based on 3 images from each of 5 samples per condition.

2.3.3. Mechanical characterization

Compressive and tensile properties of MeTro gels were assessed using a mechanical tester (Instron Model 5542) with a 10 N load cell. For compression tests, MeTro gels were prepared as described previously for swelling ratio measurements. Hydrogels were swelled for 4 h in PBS prior to mechanical testing. A digital caliper was used to measure the thickness (1 ± 0.2 mm) and diameter (5 ± 0.3 mm) of each hydrogel. Cyclic uniaxial compression tests in an unconfined state were then performed using a cross speed of 30 μm/s and a 60% strain level according to previously described procedures [18,25]. Hydrogels were cyclically preconditioned for 7 cycles after which they were subjected to another loading and unloading. The compression (mm) and load (N) were then recorded at the 8th cycle using Bluehill software. The tangent slope of the linear region of the stress–strain curve for the 8th cycle was reported as the compressive modulus. The energy loss for the 8th cycle was also calculated based on the area between the loading and unloading curves. The effects of methacrylation degree and MeTro concentration on the compressive properties of MeTro gels were determined by using various concentrations of MeTro solutions (5, 10, 5% (w/v)) with varying methacrylation degrees (31%, 44%, and 48%). At least 5 samples were tested for each condition.

For tensile tests, samples that were 20 ± 0.3 mm in length, 4 ± 0.3 mm in width, and 1 ± 0.1 mm in thickness were prepared following the procedure described previously for hydrogel fabrication. The gels were swelled for 4 h in PBS and then mounted onto the mechanical tester. The tensile grips were covered with fine sand paper to eliminate slippage. The test was performed at 1 mm/min strain rate until failure. The tensile properties of samples including elastic modulus (the tangent slope of the stress–strain curve), ultimate stress (stress at failure), and maximum strain or extensibility (strain level at failure) were reported. The effect of methacrylation degree and MeTro concentration on tensile properties of hydrogels were investigated. In addition, the extensibilities of native pulmonary artery and aorta of sheep were obtained to compare with the strain failure of the fabricated MeTro gel. At least 5 gels were tested per condition.

2.4. In vitro studies

2.4.1. Cell culture

Immortalized green fluorescent protein (GFP)-expressing human umbilical vein endothelial cells (HUVEC; ATCC) and NIH 3T3 fibroblasts were used in this study. HUVECs were cultured in a 5% CO_2 humidified incubator at 37 °C in endothelial basal

medium (EBM-2; Lonza) supplemented with endothelial growth BulletKit (Lonza) and 100 units/ml penicillin-streptomycin (Gibco, USA). 3T3 fibroblast cells were maintained in Dulbecco's modified eagle medium (DMEM; Invitrogen) modified with 10% fetal bovine serum (FBS) and 100 units/ml penicillin-streptomycin. Cells were passaged approximately 2 times per week and media was changed every 2 days.

2.4.2. Surface seeding (2D culture)

For cell adhesion and proliferation studies, MeTro gels were made following exposure to 6.9 mW/cm^2 UV light (360–480 nm) for 35 s on 3-(trimethoxysilyl) propyl methacrylate (TMSPMA, Sigma) treated glass. The slides containing MeTro were seeded with cells (2×10^5 cells/scaffold) and incubated for 7 days. Media were changed every second day.

2.4.3. Cell viability

Cell viability was determined by using a Live/Dead assay Kit (Invitrogen, USA) according to the manufacturer's instructions. To perform cell viability assay, the cells were stained with 0.5 μl/ml calcein AM and 2 μl/ml ethidium homodimer-1 (EthD-1) in PBS. Two hundred μl calcein AM/(EthD-1) solution was added to each well of a 24 well plate containing hydrogels. The well plate was then incubated at 37 °C for 20 min after which the live (green) and dead (red) cells were observed by using an inverted fluorescence microscope (Nikon TE 2000-U, Nikon instruments Inc., USA). The number of live and dead cells was counted by ImageJ software using at least 4 images from different areas of 3 gels for each condition. Cell viability was then calculated based on the number of live cells divided by the total cell number.

2.4.4. Cell adhesion, proliferation, and spreading

Rhodamine-phalloidin (Alexa-Fluor 594; Invitrogen) and 4′,6-diamidino-2-phenylindole (DAPI; Sigma) staining was used to investigate cellular attachment, proliferation, and spreading on the surfaces of fabricated hydrogels. For DAPI staining, the cell-seeded scaffolds were first fixed in 4% (v/v) paraformaldehyde (Electron Sciences) solution in PBS for 30 min. The samples were then incubated in a 0.1% (v/v) DAPI solution in PBS for 10 min at 37 °C to stain the cell nuclei. The stained samples were then washed twice with PBS before visualizing with an inverted fluorescence microscope. ImageJ software was used to count the DAPI stained nuclei and assess the proliferation of the cells on the surfaces of gels at various culture times. To stain F-actin filaments of the cell, cell-seeded gels were fixed in 4% (v/v) paraformaldehyde for 30 min. The cells were then permeabilized in a 0.1% (w/v) Triton X-100 solution in PBS for 20 min and blocked in 1% (w/v) bovine serum albumin (BSA) for 1 h. The samples were then incubated in a solution of 1:40 ratio of Alexa Fluor-594 phalloidin in 0.1% BSA for 45 min at room temperature to stain the actin cytoskeleton.

2.4.5. Cell encapsulation (3D culture)

Cells were trypsinized and resuspended in MeTro solution containing 0.5% (w/v) photoinitiator at a concentration of 5×10^6 cells/ml. Cell-laden MeTro gels were made following exposure to 6.9 mW/cm^2 UV light (360–480 nm) for 35 s on TMSPMA treated glass. The gels were then washed 3 times with PBS and incubated for 7 days in 3T3 medium in a culture incubator at 37 °C.

2.5. Statistical analysis

Data were compared using one-way ANOVA followed by Bonferroni's post-hoc test (GraphPad Prism 5.02) software. Error bars represent the mean ± standard deviation (SD) of measurements ($^*p < 0.05$, $^{**}p < 0.01$, and $^{***}p < 0.001$).

3. Results and discussion

In this study, we synthesized MeTro gels with tunable physical properties, which can be used in both 3D elastic environments for cell encapsulation and 2D films for cellular attachment and growth. These hydrogels can be made in a variety of shapes and sizes, and present several advantages over other elastin-derived hydrogels and synthetic elastomers. First, MeTro gels are formed rapidly within 35 s, which is shorter than the typical time (~24 h) required to chemically crosslink elastin-based hydrogels [15,17]. Second, the photocrosslinking of MeTro gels in aqueous solution eliminates the use of toxic crosslinkers [15,25] and organic solvents [18] during the hydrogel synthesis. Third, the potential to directly encapsulate cells rapidly within the MeTro gels allows for a pronounced cell distribution throughout the matrix. This would allow to overcome problems associated with minimal cell penetration into 3D matrices post-casting due to common issues such as low porosity, pore connectivity and small pore sizes [15,17]. Fourth, unlike other synthetic elastomers such as polyurethane [33], the use of biodegradable MeTro gels do not cause cytotoxicity through *in vivo* degradation, as the gels are formed from a human protein. Fifth, tropoelastin-based materials are more stable [15] compared to some biodegradable elastomers such as poly(glycerol-sebacate) (PGS) [34], thus providing mechanical support until new tissues form. Sixth, the presence of the full secreted tropoelastin amino acid sequence including the cell-interactive C-terminus imparts cell-interactive functions to the MeTro gels by providing endogenous integrin αVβ3 cell-binding sites [35].

We first investigated the effect of methacrylation on the coacervation behavior and secondary structure of tropoelastin. Then, we used MeTro prepolymers with varying extents of methacrylation to form elastic hydrogels with tunable physical properties. The effects of methacrylation degree and polymer concentration on the pore characteristics, swelling ratios, and mechanical properties (both tensile and compressive behaviors) of fabricated hydrogels were studied. In addition, we demonstrated functional performance for two cell types (HUVECs, and 3T3 fibroblasts) in supporting their growth on and embedded within MeTro hydrogels.

3.1. Synthesis of MeTro

MeTro was synthesized using recombinant human tropoelastin [36] and methacrylic anhydride. The degree of methacrylate functionalization was controlled by specific methacrylic anhydride concentrations and was quantified by ^{1}H NMR analysis (Fig. 1A). MeTro polymers with methacrylation degrees of 31%, 44%, and 48% were produced with 8% (v/v), 15% (v/v), and 20% (v/v) methacrylic anhydride, respectively. The resultant MeTro solutions were lyophilized prior to use. To confirm the integrity of MeTro, we assessed the effect of methacrylation on secondary structure and functional protein performance by coacervation. Coacervation of tropoelastin is an inverse temperature transition process of massive protein assembly that plays a critical role in elastin formation. This temperature transition is mainly due to the intermolecular hydrophobic association of tropoelastin molecules in an aqueous environment and so is sensitive to protein concentration, pH, salt, and impurities [37]. On this basis, acrylate modification at lysine residues increased the protein's hydrophobicity and gave a lower coacervation temperature (Fig. 1B). CD spectra of tropoelastin and MeTro each displayed an intense negative band at 200 nm, consistent with substantial secondary disorder, and a shoulder centered at 222 nm, demonstrating the presence of α-helical structure each of which is normal for tropoelastin [36,38] (Fig. 1C). Quantification of secondary structure revealed that methacrylation of tropoelastin did not significantly alter the secondary structure of the protein (Fig. 1D). The secondary structure calculated for all samples were approximately 12% α-helix, 18% β-sheet, 13% β-turn, 9% polyproline type-II turn and 48% unresolved, which are similar to those reported for bovine tropoelastin [39] and elastin [40].

3.2. Fabrication and physical properties of MeTro hydrogels

Highly elastic and porous 3D MeTro hydrogels were prepared by UV irradiation (6.9 mW/cm^2) of MeTro prepolymer solutions for 35 s. Average pore size, swelling ratio, and mechanical performance were tailored by varying both the extent of methacrylation and MeTro concentration.

We found that the methacrylation degree significantly influenced both pore characteristics and swelling behavior of fabricated hydrogels. The average pore size of 10% (w/v) MeTro gels decreased from 51 ± 9 μm to 23.4 ± 5.8 μm and 11.7 ± 3.3 μm as the methacrylation degree was increased from 31% to 44% and 48%,

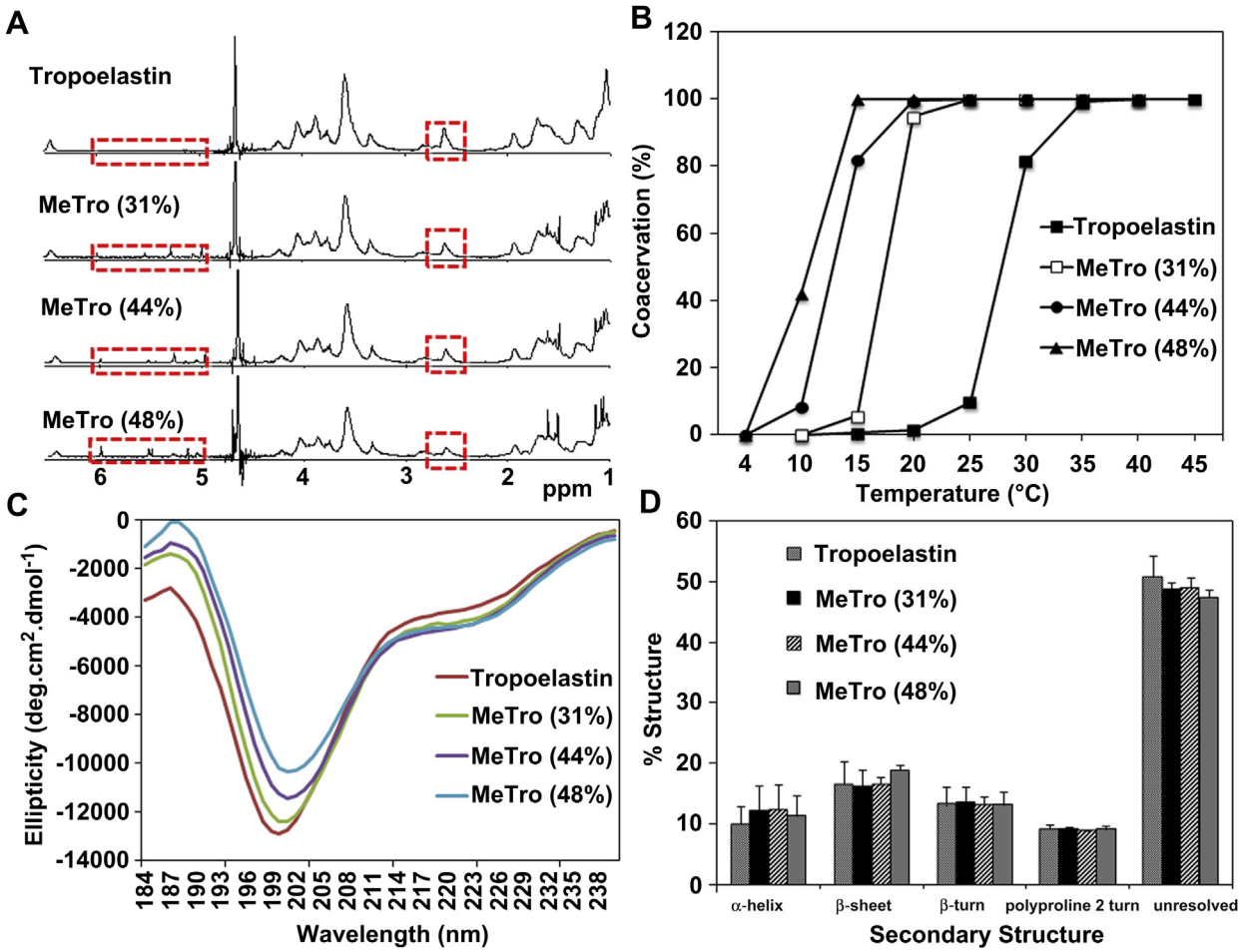

Fig. 1. Effect of methacrylation on tropoelastin. (A) Representative ^{1}H NMR spectrum of tropoelastin and MeTro solutions in D_2O measured at 4 °C. The methacrylation degree of MeTro is provided in parentheses. Peaks that correspond to methacrylate groups (between 4.9 and 6 ppm) grew in intensity at the expense of the lysine-specific peak in tropoelastin at 2.6 ppm. (B) Coacervation curves for tropoelastin and MeTro with different degrees of methacrylation, the coacervation temperature decreased with increasing methacrylation. (C) CD spectra of tropoelastin and MeTro with indicated amounts of methacrylation. (D) Percent calculated secondary structure derived from CD data, indicating that methacrylation had no discernible effect on the secondary structure of tropoelastin.

respectively (Fig. 2Ai–iv) ($P < 0.01$). In addition, swelling ratios decreased from 4.1 ± 0.3 to 2.3 ± 0.3 and 1.2 ± 0.2 g PBS/g protein as the degree of methacrylation was increased from 31% to 44% and 48%, respectively (Fig. 2Av). On this basis, higher degrees of methacrylation are likely to enhance the crosslinking density, and lead to reduced pore sizes and swelling ratio of the resulting MeTro gels.

In contrast we found that protein concentration had no effects on the swelling ratios and pore architectures of the hydrogels as shown in Fig. 2B. All MeTro gels made using various concentrations of MeTro (5, 10, 15% (w/v)) at 31% methacrylation contained large pores (44 μm–63.5 μm) on their surfaces and within gel cross-sections (Fig. 2Bi–vii), conducive to nutrient and oxygen diffusion as well as removal of metabolic waste in 3D constructs.

The mechanical characteristics of MeTro hydrogels were analyzed by tensile and unconfined cyclic compression tests. Our fabricated material exhibited superior mechanical properties compared to other photocrosslinkable gels, including substantial extensibility up to 400% before rupture (Fig. 3A), reversible deformation with low energy loss, and high resilience upon stretching. The fabricated hydrogels showed soft tissue-like elastic moduli between 2.8 ± 0.6 kPa and 14.8 ± 1.9 kPa with an ultimate tensile strength ranging from 12.5 ± 2.2 kPa to 39.3 ± 2.5 kPa that was tuned by both the extent of methacrylation and MeTro concentration (Fig. 3B–E, Table 1). In addition, the extensibility of the fabricated MeTro gels was significantly decreased by increasing the methacrylation degree and polymer concentration. For example, the strain at break for a 10% (w/v) MeTro gel decreased 2.5-fold from 332 ± 48 to 135 ± 11 when the methacrylation degree was enhanced from 31% to 48%. This can be due to the enhanced degree of crosslinking in MeTro gels with higher methacrylation, which resulted in an increase in material stiffness and consequently decrease in elasticity. MeTro gels exhibited higher elastic moduli and extensibility compared to other photocrosslinkable hydrogels such as 10% (w/v) GelMA gel at 80% methacrylation [31] (modulus: 3.3 ± 0.7 kPa, extensibility: ~100%).

The extensibility of native pulmonary artery was 204 ± 9% and 158 ± 25% in the circumferential and radial directions, respectively. In addition, in longitudinal direction, the strain level of failure for aorta was 266 ± 55% and in circumferential direction was 282 ± 48%. The extensibility of fabricated MeTro gel, which ranged from 135 to 400% depending on the methacrylation degree and polymer concentration, is in the maximum strain range of native pulmonary artery and aorta. The unique elastic properties of this photocrosslinkable MeTro gel point to its potential as a suitable cell-interactive protein-based matrix for the engineering of elastic tissues such as blood vessel, skin, lung, and cardiac tissue because of the important role played by elastin in mechanical and cell-interactive functions in these tissues.

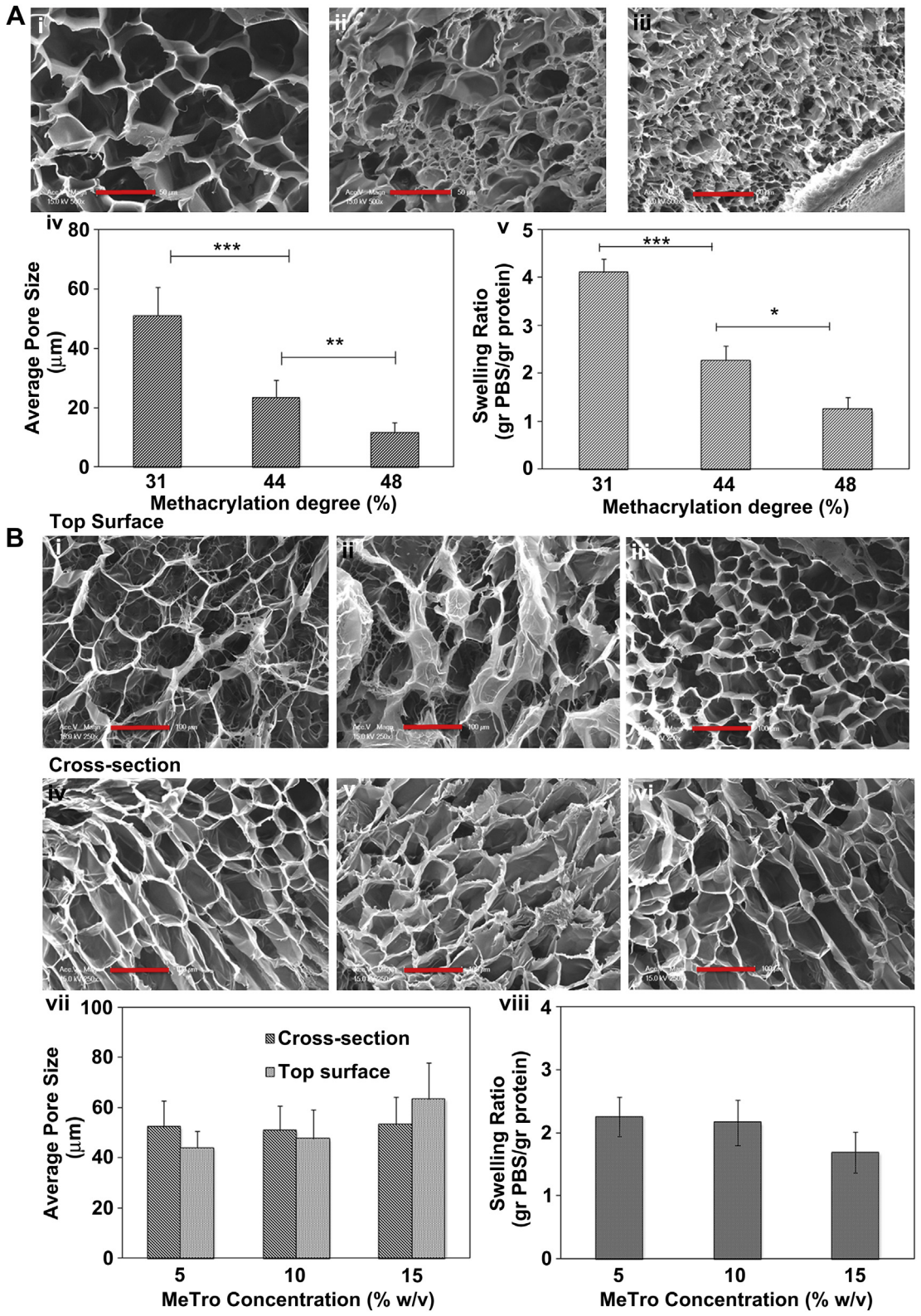

Fig. 2. Pore characteristics and equilibrium swelling properties of MeTro gels. Representative SEM images from the cross-sections of 10% (w/v) MeTro hydrogels with (Ai) 31; (Aii) 44; and (Aiii) 48% methacrylation (scale bars: 50 μm). The structures of these hydrogels became more compact with increasing methacrylation. (Aiv) Effect of methacrylation on the average pore sizes of MeTro gels, derived from SEM images ($n = 100$). (Av) Effect of methacrylation on the swelling ratio of hydrogels. SEM images of MeTro hydrogels produced by using (Bi, Biv) 5; (Bii, Bv) 10; and (Biii, Bvi) 15% (w/v) protein concentrations with 31% methacrylation. All gels have a highly porous structure. Pores are present both on the top surface and throughout the cross-section of MeTro gels. Top surfaces are shown in Bi–Biii and cross-sections in Biv–Bvi (scale bars: 100 μm). (Bvii) The average pore sizes on the top surfaces and within the cross sections of MeTro gels made with varying protein concentrations. (Bviii) Effect of protein concentration on the swelling ratios of the hydrogels.

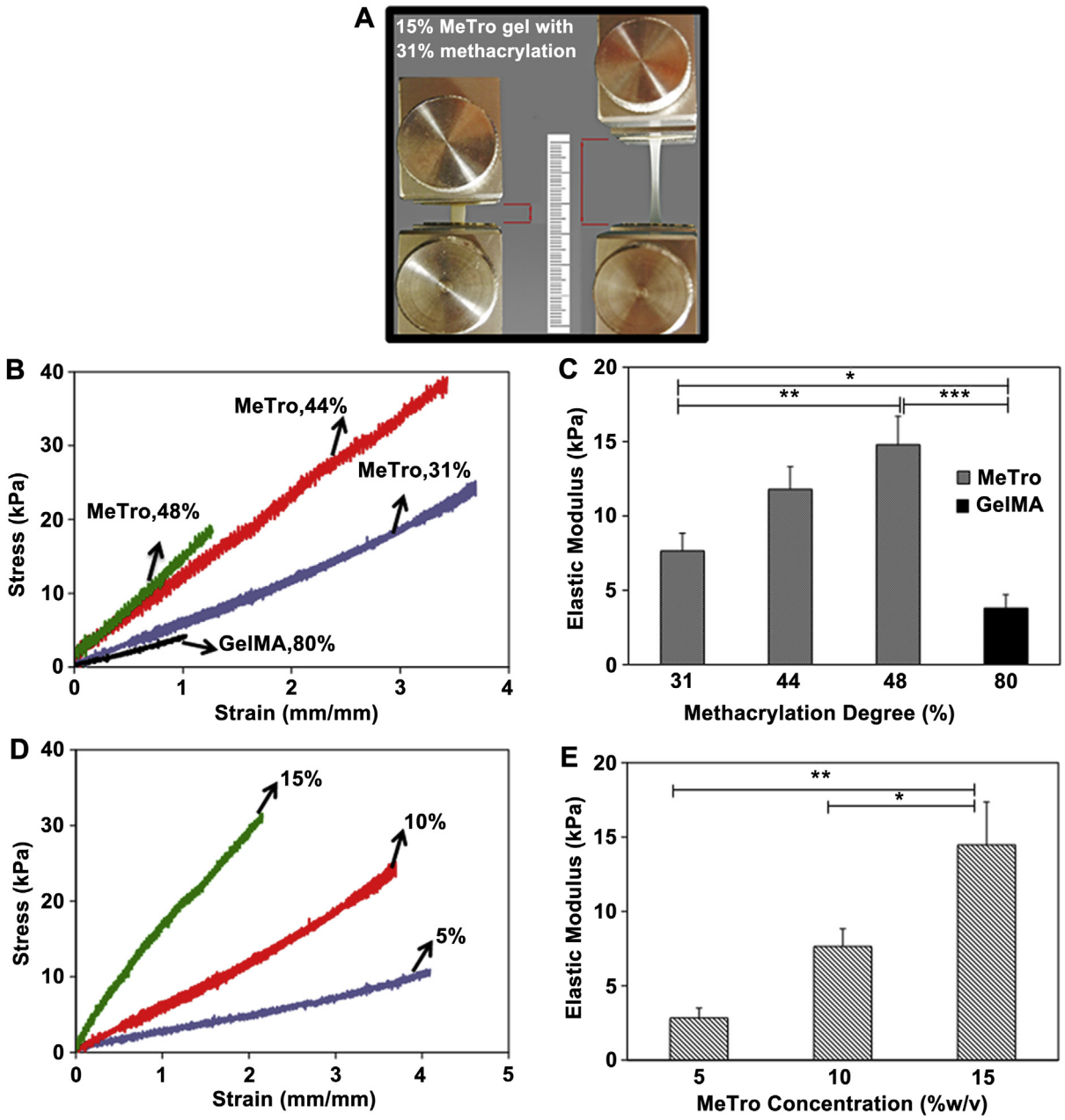

Fig. 3. Tensile properties of MeTro hydrogels. (A) Image of a 15% (w/v) MeTro gel with 31% methacrylation, before and after stretching. (B) Representative strain/stress curves and (C) elastic moduli of hydrogels produced from 10% (w/v) MeTro at varying degrees of methacrylation and 10% (w/v) GelMA with 80% methacrylation. (D) Representative strain/stress curves and (E) elastic moduli of hydrogels produced from various concentrations of MeTro with 31% methacrylation.

The compressive behavior of fabricated hydrogels was evaluated by applying cyclic compression on the hydrogels (Fig. 4). Gels deformed reversibly following 8 cycles of loading and unloading at 60% strain. The hydrogels displayed energy losses of ~24.1–30.5% depending on MeTro concentration, which is comparable to the energy loss of purified native elastin at 23 ± 10% [41]. The compressive modulus increased from 8.8 ± 0.4 to 14.8 ± 1.1 and 159.7 ± 18.8 kPa when the MeTro concentration was increased from

Table 1
Mechanical characterization of photocrosslinked MeTro hydrogels.

Methacrylation degree (%)	MeTro concentration (%w/v)	Compressive modulus (kPa)	Energy loss (%)	Elastic modulus (kPa)	Stress at break (kPa)	Strain at break (%)
31	5	8.8 ± 0.4	24 ± 7	2.8 ± 0.6	12.5 ± 2.2	402 ± 10
31	10	14.8 ± 1.1	23 ± 3.2	7.6 ± 1.19	29.4 ± 5.7	376 ± 38
31	15	159.7 ± 18.8	31 ± 6.4	14.5 ± 2.8	27.2 ± 3.4	273 ± 50
44	10	24.6 ± 4	27 ± 2.3	11.8 ± 1.5	39.3 ± 2.5	332 ± 48
48	10	26.6 ± 4.3	41 ± 3.9	14.8 ± 1.9	23.8 ± 7.5	135 ± 11

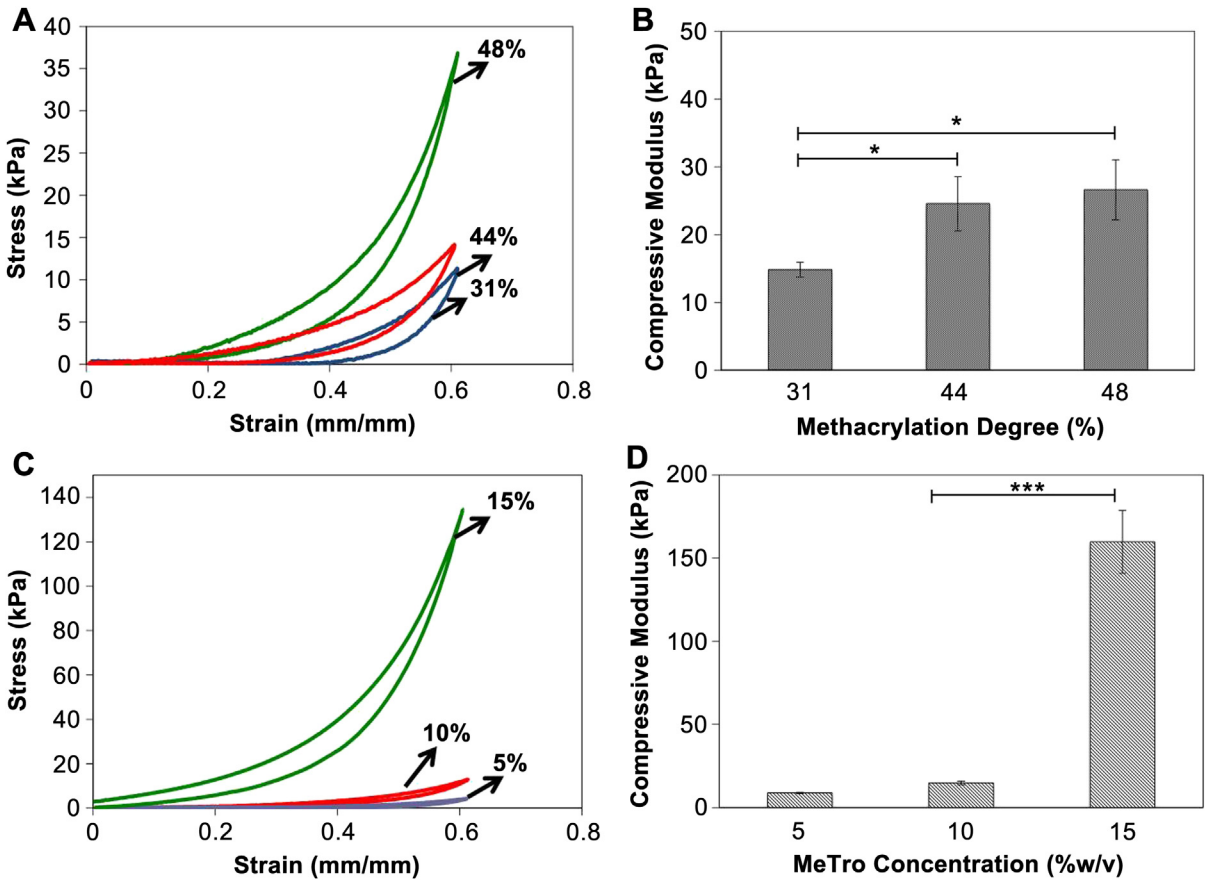

Fig. 4. Unconfined compressive behavior of MeTro gels. (A, C) Representative cyclic strain/stress curves and (B, D) compressive moduli for hydrogels produced from 10% (w/v) MeTro at (A, B) varying degrees of methacrylation; and (C, D) various concentrations of MeTro with 31% methacrylation degree. Error bars represent the SD of measurements performed on 5 samples ($^{*}p < 0.05$, $^{**}p < 0.01$, $^{***}p < 0.001$).

5 to 10 and 15% (w/v). The high compressive modulus of 15% (w/v) MeTro gel is likely due to the increased viscosity of this higher protein concentration prepolymer solution which gave rise to an enhanced crosslinking density within the fabricated hydrogels after exposure to UV. In contrast, the low concentration of the 5% (w/v) MeTro prepolymer solution limited the UV crosslinking of the solution, which resulted in the formation of hydrogels with lower compressive modulus.

It is likely that the compression data were dominated by the packing density of tropoelastin molecules. In contrast, extensional behavior is a complex combination of crosslinking density and extensibility of the constituent tropoelastin components. On this basis the compressive modulus showed a marked dependence on concentration as evidenced by sharp increase between 10% (w/v) and 15% (w/v) gels.

In addition, cyclic loading and unloading had no effect on the stiffness of the gels and all of the hydrogels fully recovered immediately after each unloading without any permanent deformation. Most other hydrogels exhibit high hysteresis and permanent deformation after unloading. For example, in a recent study highly stretchable hybrid alginate/polyacrylamide gels weaken by their second loading but somewhat recover if that loading is delayed by a day [13]. The elasticity and recoverable energy dissipation in our material is dictated by water interactions with repeated hydrophobic regions in tropoelastin while hydrophilic domains are responsible for crosslinking. On stretching, exposed hydrophobic domains organize structured water and lead an entropic drive to mechanical collapse; in this way the hydrophobic regions contract upon unloading, leading to recovery. MeTro gels have higher compressive moduli over elastin-based gels that use a variety of crosslinks and also other photocrosslinkable hydrogels [1,31,32,42,43], making it a unique, stretchable human protein-based gel that can be considered for the repair of elastic tissues.

3.3. Cell interactions with MeTro hydrogels

MeTro gels with 10% (w/v) protein concentration and 31% methacrylation degree were used to examine the cell-interactive capabilities (e.g. cell viability, adhesion, spreading, and proliferation) of the resulting hydrogels. We used HUVECs and 3T3 fibroblasts as model cells. Cells were cultured for a week on the surfaces of MeTro hydrogels. Cellular viability, adhesion, spreading, and proliferation on the hydrogels were examined by using calcein-AM/ethidium homodimer Live/Dead assay, SEM analysis, and F-actin/DAPI staining, respectively. As shown in Fig. 5M, cell viability was >92% for MeTro gels seeded with fibroblasts (Fig. 5A–C) and HUVECs (Fig. 5D–F) over a 7-day culture. In addition, fibroblasts (Fig. 5G) and endothelial cells (Fig. 5H) adhered to and formed monolayers on the surfaces of MeTro hydrogels; however, cells did not grow on the control PEG hydrogel (Fig. 5I and L). These cells had spread as indicated by the staining of cell F-actin filaments and nuclei with rhodamine-phalloidin/DAPI (Fig. 5J–K). The capacity of MeTro gel surfaces to support cell proliferation was evidenced by the increasing number of DAPI stained nuclei per given hydrogel area during culture (Fig. 5N). These results demonstrated the capacity for fabricated MeTro gels to act as cell-interactive substrates

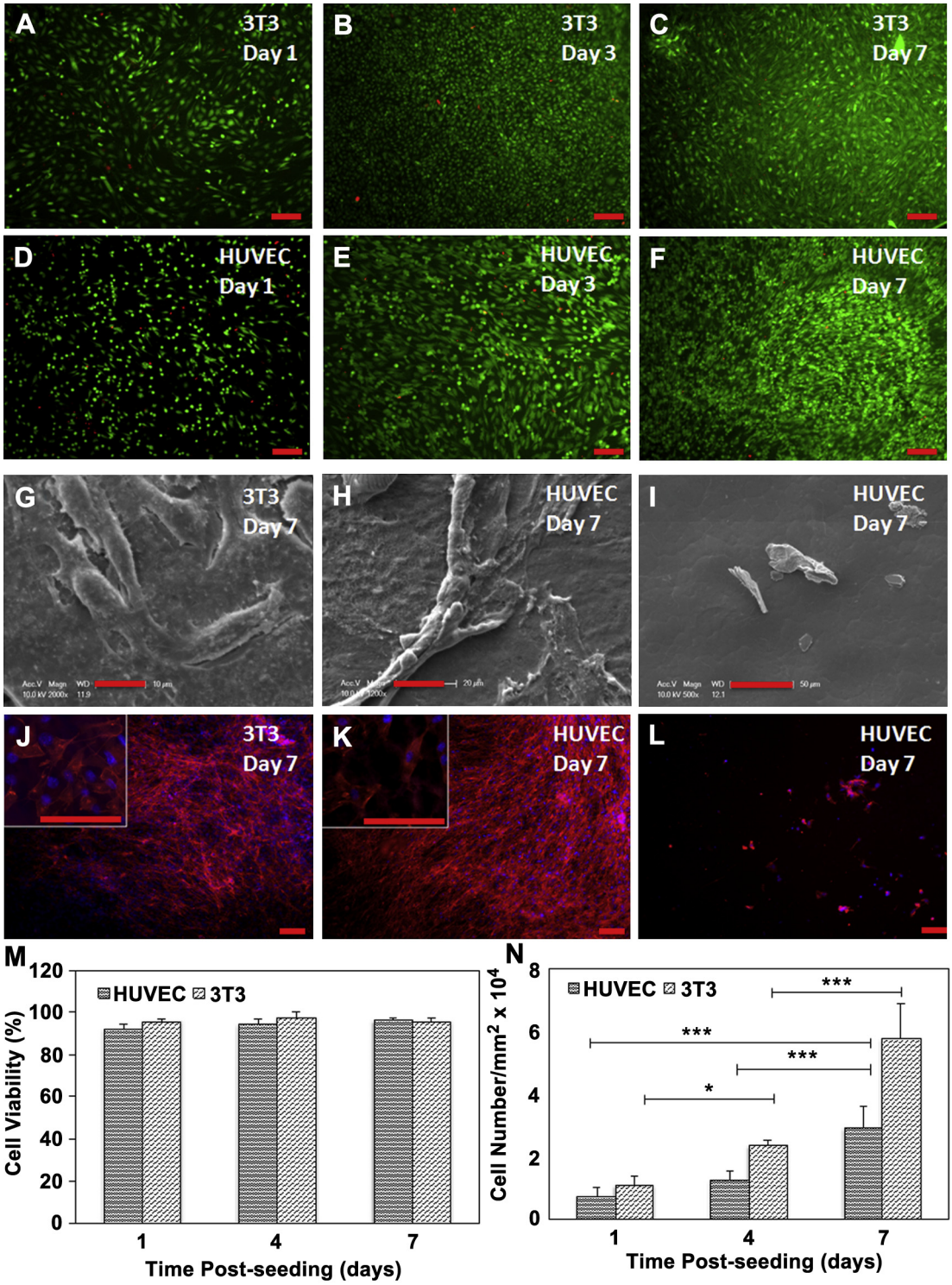

Fig. 5. 2D studies in vitro on MeTro hydrogels. Live/Dead images from the surfaces of MeTro hydrogels seeded with (A–C) 3T3 and (D–F) HUVECs on days 1, 4, and 7 of culture (scale bar = 100 μm). MeTro gels were produced using 10% (w/v) MeTro with 31% methacrylation. Representative SEM image from the top surface of MeTro hydrogels seeded with (G) 3T3, and (H) HUVECs, taken on day 7 of culture, indicating that cell readily adhered to the surfaces of the fabricated hydrogels (scale bar = 20 μm). (I) SEM image from the surface of a HUVEC-seeded PEG gel as control (scale bar = 20 μm). Rhodamine-labeled phalloidin/DAPI staining for F-actin/cell nuclei of MeTro gels seeded with (J) 3T3, and (K) HUVECs, and (L) a PEG hydrogel seeded with HUVECs following 7 days of culture (scale bar = 100 μm). (M) Quantification of cell viabilities 1, 4, and 7 days after cell seeding. (N) Cell densities, defined as the number of DAPI stained nuclei per given hydrogel area, increasing over the culture time, demonstrating cell proliferation on MeTro gel surfaces ($^{*}p < 0.05$, $^{***}p < 0.001$).

with applications for the formation of 2D films or coating agent. The excellent cell-interactive properties of MeTro gels are likely due to integrin-based cell-binding sites within the tropoelastin molecules [35].

The viability of 3T3 fibroblasts encapsulated within the 3D structures of highly elastic MeTro gels was investigated over a 7-day culture. As shown in Fig. 6A–D, when 3T3 fibroblasts were encapsulated within the 3D structure of 10 and 15% (w/v) MeTro

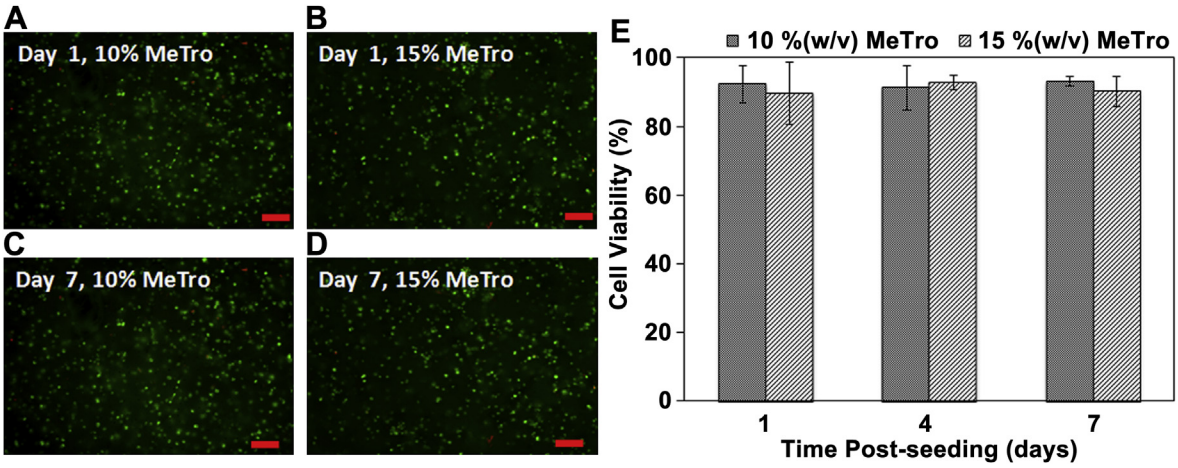

Fig. 6. 3D in vitro studies on MeTro hydrogels. 3T3 fibroblasts embedded in 3D MeTro gels were stained with calcein AM (green)/ethidium homodimer (red) Live/Dead assay, Live/Dead images from 3T3 cells encapsulated within (A, C) 10% (w/v), and (B, D) 15% (w/v) MeTro gels on day 1(A, B) and 7 (C, D) of culture (scale bar = 100 μm). (E) Quantification of cell viability 1, 4, and 7 days after encapsulation (MeTro with 31% methacrylation was used for hydrogel fabrication). (For interpretation of the references to color in this figure legend, the reader is referred to the web version of this article.)

hydrogels with 31% methacrylation, they remained viable for at least a week in culture (Fig. 6E). This demonstrated the compatibility of this range of MeTro gels with 3D cell encapsulation. To our best knowledge, this is the first highly elastic human protein-based hydrogel that is able to embed viable cells within its 3D structures.

We have previously fabricated elastin-based hydrogels through chemical crosslinking of tropoelastin and soluble elastin using various types of crosslinking agents such as hexamethylene diisocyanate [18], glutaraldehyde [25], and bis(sulfosuccinimidyl) suberate [15]. In all these formulations, cells were seeded on the surfaces of the materials after hydrogel formation, as the use of toxic crosslinkers did not allow for cell embedding prior to hydrogel formation. Limited cellular penetration and growth within 3D structures of these gels [15] were the main limitations for tissue engineering applications. Electrospinning techniques [26] and dense gas carbon dioxide [17,18] were used to enhance the pore sizes and consequently facilitate cell penetration and infiltration into the 3D structures of these elastin-based biomaterials. However, the non-homogenous cellular distribution within these elastic gels was an issue. The MeTro gel developed in this study overcomes these limitations and introduces a new class of bioelastomer with tunable elasticity and the capacity for cell encapsulation in a 3D elastic environment.

Due to these unique properties, MeTro hydrogels can serve as suitable biomaterials for engineering diverse elastic tissues where elasticity plays an important role in their functions. MeTro confers the additional advantages of viable cell encapsulation within 3D hydrogels while allowing for functional, cell surface colonization. This is the first report of a cytocompatible, elastic tissue equivalent with excellent mechanical properties and cell-interactive behavior.

4. Conclusion

In this study, we demonstrated the construction of a cell-laden human protein-based hydrogel, MeTro. The extraordinary properties of MeTro gels include high extensibility, recoverability upon loading and unloading, ability for fast polymerization, an easy method of synthesis, and suitability for both 3D cell encapsulation and 2D cell seeding. These features point out that MeTro constructs are a unique class of materials for various tissue engineering applications that rely on elasticity while allowing for cell encapsulation and surface growth. In many applications including the engineering of elastic tissues, the use of hydrogels is often severely limited by their low mechanical properties and stretchability. Compromised mechanical properties of hydrogels for cell encapsulation can lead to unintended cell release and death, while low toughness limits durability. Consequently, hydrogels of superior stiffness, extensibility, and recoverability are likely to improve performance in these applications.

Author contributions

N.A. and S.M.M. designed the experiments and wrote the paper. N.A. and S.M.M performed experiments and analyzed the data. P.Z. performed experiments. G.C.U. revised the manuscript. A.S.W. and A.K. provided conceptual input, designed experiments, and revised the paper.

Acknowledgments

N.A. acknowledges the support from the National Health and Medical Research Council. A.K. acknowledges funding from the National Science Foundation CAREER Award (DMR 0847287), the office of Naval Research Young National Investigator Award, the National Institutes of Health (HL092836, DE019024, EB012597, AR057837, DE021468, HL099073, EB008392), and the Presidential Early Career Award for Scientists and Engineers (PECASE). A.S.W. acknowledges funding from the Australian Research Council, Australian Defense Health Foundation, National Health & Medical Research Council and National Institutes of Health (EB014283). A.S.W. is the Scientific Founder of Elastagen Pty Ltd. The authors declare no conflict of interest in this work.

References

[1] Chen Y-C, Lin R-Z, Qi H, Yang Y, Bae H, Melero-Martin JM, et al. Functional human vascular network generated in photocrosslinkable gelatin methacrylate hydrogels. Adv Func Mater 2012;22:2027–39.
[2] Khademhosseini A, Langer R. Microengineered hydrogels for tissue engineering. Biomaterials 2007;28:5087–92.
[3] Peppas NA, Hilt JZ, Khademhosseini A, Langer R. Hydrogels in biology and medicine: from molecular principles to bionanotechnology. Adv Mat 2006;18:1345–60.
[4] Ward R, Jones R. Polyurethanes and silicone polyurethane copolymers. In: Paul D, editor. Comprehensive biomaterials. Oxford: Elsevier; 2011. p. 431–77.
[5] Chen Q, Liang S, Thouas GA. Elastomeric biomaterials for tissue engineering. Prog Polym Sci 2013;38:584–671.

[6] McBane JE, Sharifpoor S, Cai K, Labow RS, Santerre JP. Biodegradation and *in vivo* biocompatibility of a degradable, polar/hydrophobic/ionic polyurethane for tissue engineering applications. Biomaterials 2011;32:6034–44.
[7] Yu J, Takanari K, Hong Y, Lee K-W, Amoroso NJ, Wang Y, et al. Non-invasive characterization of polyurethane-based tissue constructs in a rat abdominal repair model using high frequency ultrasound elasticity imaging. Biomaterials 2013:2701–9.
[8] Hazer DB, Kilicay E, Hazer B. Poly(3-hydroxyalkanoate)s: diversification and biomedical applications: a state of the art review. Mater Sci Eng C 2012;32:637–47.
[9] Rai R, Keshavarz T, Roether JA, Boccaccini AR, Roy I. Medium chain length polyhydroxyalkanoates, promising new biomedical materials for the future. Mater Sci Eng R Rep 2011;72:29–47.
[10] Webb AR, Kumar VA, Ameer GA. Biodegradable poly(diol citrate) nanocomposite elastomers for soft tissue engineering. J Mater Chem 2007;17:900–6.
[11] Engelmayr GC, Cheng M, Bettinger CJ, Borenstein JT, Langer R, Freed LE. Accordion-like honeycombs for tissue engineering of cardiac anisotropy. Nat Mater 2008;7:1003–10.
[12] Wang Y, Ameer GA, Sheppard BJ, Langer R. A tough biodegradable elastomer. Nat Biotech 2002;20:602–6.
[13] Sun J-Y, Zhao X, Illeperuma WRK, Chaudhuri O, Oh KH, Mooney DJ, et al. Highly stretchable and tough hydrogels. Nature 2012;489:133–6.
[14] Lv S, Dudek DM, Cao Y, Balamurali MM, Gosline J, Li H. Designed biomaterials to mimic the mechanical properties of muscles. Nature 2010;465:69–73.
[15] Mithieux SM, Rasko JEJ, Weiss AS. Synthetic elastin hydrogels derived from massive elastic assemblies of self-organized human protein monomers. Biomaterials 2004;25:4921–7.
[16] Mithieux SM, Tu Y, Korkmaz E, Braet F, Weiss AS. In situ polymerization of tropoelastin in the absence of chemical cross-linking. Biomaterials 2009;30:431–5.
[17] Annabi N, Mithieux SM, Weiss AS, Dehghani F. The fabrication of elastin-based hydrogels using high pressure CO_2. Biomaterials 2009;30:1–7.
[18] Annabi N, Mithieux SM, Boughton EA, Ruys AJ, Weiss AS, Dehghani F. Synthesis of highly porous crosslinked elastin hydrogels and their interaction with fibroblasts *in vitro*. Biomaterials 2009;30:4550–7.
[19] Annabi N, Fathi A, Mithieux SM, Martens P, Weiss AS, Dehghani F. The effect of elastin on chondrocyte adhesion and proliferation on polycaprolactone/elastin composites. Biomaterials 2011;32:1517–25.
[20] MacEwan SR, Chilkoti A. Elastin-like polypeptides: biomedical applications of tunable biopolymer. Pept Sci 2012;94:60–77.
[21] Betre H, Ong SR, Guilak F, Chilkoti A, Fermor B, Setton LA. Chondrocytic differentiation of human adipose-derived adult stem cells in elastin-like polypeptide. Biomaterials 2006;27:91–9.
[22] McHale MK, Setton LA, Chilkoti A. Synthesis and *in vitro* evaluation of enzymatically crosslinked elastin-like polypeptide gels for cartilaginous tissue repair. Tissue Eng 2006;11:1768–79.
[23] Lim DW, Nettles DL, Setton LA, Chilkoti A. In situ crosslinking of elastin-like polypeptide block copolymers for tissue repair. Biomacromolecules 2008;9:222–30.
[24] McHale Melissa K, Setton Lori A, Chilkoti A. Synthesis and in vitro evaluation of enzymatically cross-linked elastin-like polypeptide gels for cartilaginous tissue repair. Tissue Eng 2005;11:1768–79.
[25] Annabi N, Mithieux SM, Weiss AS, Dehghani F. Cross-linked open-pore elastic hydrogels based on tropoelastin, elastin and high pressure CO_2. Biomaterials 2010;31:1655–65.
[26] Rnjak-Kovacina J, Wise SG, Li Z, Maitz PKM, Young CJ, Wang Y, et al. Tailoring the porosity and pore size of electrospun synthetic human elastin scaffolds for dermal tissue engineering. Biomaterials 2011;32:6729–36.
[27] Raphel J, Parisi-Amon A, Heilshorn SC. Photoreactive elastin-like proteins for use as versatile bioactive materials and surface coatings. J Mater Chem 2012;22:19429–37.
[28] Wu WJ, Vrhovski B, Weiss AS. Glycosaminoglycans mediate the coacervation of human tropoelastin through dominant charge interactions involving lysine side chains. J Biol Chem 1999;274:21719–24.
[29] Martin SL, Vrhovski B, Weiss AS. Total synthesis and expression in *Escherichia coli* of a gene encoding human tropoelastin. Gene 1995;154:159–66.
[30] Sreerama N, Woody RW. Estimation of protein secondary structure from circular dichroism spectra: comparison of CONTIN, SELCON, and CDSSTR methods with an expanded reference set. Anal Biochem 2000;287:252–60.
[31] Nichol JW, Koshy ST, Bae H, Hwang CM, Yamanlar S, Khademhosseini A. Cell-laden microengineered gelatin methacrylate hydrogels. Biomaterials 2010;31:5536–44.
[32] Hutson CB, Nichol JW, Aubin H, Bae H, Yamanlar S, Al-Haque S, et al. Synthesis and characterization of tunable poly(ethylene glycol): gelatin methacrylate composite hydrogels. Tissue Eng 2011;17:1713–23.
[33] Miyagawa S, Roth M, Saito A, Sawa Y, Kostin S. Tissue engineered cardiac constructs for cardiac repair. Ann Thorac Surg 2011;91:320–9.
[34] Giraud M, Armbruster C, Carrel T, Tevaearai H. Current state of the art in myocardial tissue engineering. Tissue Eng 2007;13:1825–36.
[35] Bax DV, Rodgers UR, Bilek MM, Weiss AS. Cell adhesion to tropoelastin is mediated via the C-terminal GRKRK motif and integrin $\alpha V\beta 3$. J Biol Chem 2009;284:28616–23.
[36] Baldock C, Oberhauser AF, Ma L, Lammie D, Siegler V, Mithieux SM, et al. Shape of tropoelastin, the highly extensible protein that controls human tissue elasticity. Proc Natl Acad Sci U S A 2011;108:4322–7.
[37] Vrhovski B, Jensen S, Weiss AS. Coacervation characteristics of recombinant human tropoelastin. Eur J Biochem 1997;250:92–8.
[38] Dyksterhuis LB, Carter EA, Mithieux SM, Weiss AS. Tropoelastin as a thermodynamically unfolded premolten globule protein: the effect of trimethylamine N-oxide on structure and coacervation. Arch Biochem Biophys 2009;487:79–84.
[39] Debelle L, Alix AJP. Optical spectroscopic determination of bovine tropoelastin molecular model. J Mol Struct 1995;348:321–4.
[40] Debelle L, Alix AJP, Wei SM, Jacob M-P, Huvenne J-P, Berjot M, et al. The secondary structure and architecture of human elastin. Eur J Biochem 1998;258:533–9.
[41] Bellingham CM, Lillie MA, Gosline JM, Wright GM, Starcher BC, Bailey AJ, et al. Recombinant human elastin polypeptides self-assemble into biomaterials with elastin-like properties. Biopolymers 2003;70:445–55.
[42] Xiao W, He J, Nichol JW, Wang L, Hutson CB, Wang B, et al. Synthesis and characterization of photocrosslinkable gelatin and silk fibroin interpenetrating polymer network hydrogels. Acta Biomater 2011;7:2384–93.
[43] Bae H, Ahari AF, Shin H, Nichol JW, Hutson CB, Masaeli M, et al. Cell-laden microengineered pullulan methacrylate hydrogels promote cell proliferation and 3D cluster formation. Soft Matter 2011;7:1903–11.